ION MASS SPECTRA IN
THE IONOSPHERIC E REGION

Technical Report
CPRL Report 7-67

National Aeronautics and Space Administration
Grant: NGR-14-005-097

CHARGED PARTICLE RESEARCH LABORATORY
DEPARTMENT OF ELECTRICAL ENGINEERING
UNIVERSITY OF ILLINOIS
URBANA, ILLINOIS, 61801

TABLE OF CONTENTS

I. INTRODUCTION

This report is to comment on progress to date on research being conducted under NASA Grant NGR-14-005-097. Since the work being conducted with this support is closely related to previous work performed under supplement 3 to NASA Grant NSG-511 no attempt is made to distinguish between them and all progress is contained in this report. In general, the work related to the payloads intended for launch from Wallops Island was supported by supplement 3 to Grant NSG-511. The remainder was supported by Grant NGR-14-005-097.

In brief, the major purpose of the grants was to support the development of a mass spectrometer package for use in ionospheric studies utilizing Nike-Apache rockets. The hope then was that a series of rocket launchings would follow to investigate the behavior of the ionosphere under varying conditions. The details of the requirements are included in the appendix. This appendix consists of a thesis written by a masters degree candidate.

II. WORK COMPLETED

A mass spectrometer was developed and two rocket payloads were constructed in cooperation with GCA Corporation, a holder of a concurrent contract with NASA. The laboratory tests were conducted and sample spectra obtained during these tests are included in the appendix. The entire payload performed quite well during these tests and no problems developed during the entire test program.

Two launches were scheduled for August 24, 1966, from the Wallops Island facility. Only one of the payloads was launched when it became clear that the spectrometer package had a malfunction during the flight of the first payload. The trouble appeared to be high voltage breakdown at some point in the package. There also appeared to be some interference between experiments.

Further laboratory tests confirmed that high voltage breakdown in the multiplier could in fact result in outputs similar to those recorded during the launch of the first payload. Further testing should have been carried out in the laboratory but a commitment to launch two payloads from Rio Grande, Brazil, on November 12, 1966, during a solar eclipse was already becoming tight timewise.

It was believed that the difficulties could be remedied by taking the following steps:

1) Reduce the voltage applied to the electron multiplier.
2) Provide ports on the quadrupole and multiplier compartments to facilitate pumping down during flight.

3) Enlarging the entrance and exit apertures of the quadrupole to compensate for the gain lost by reducing the multiplier voltages.

4) Shielding supply leads to cut down interference.

To facilitate incorporation of General Mendonca's experiment on the Brazil shots the quadrupole structure was also lengthened to almost double its original length. A modest change to allow the measurement of total ion density was also made. This change was made to allow more precise in-flight calibration of the instrument.

Two payloads were constructed, with GCA Corporation, incorporating these changes for use during the Brazil expedition.

Upon launching the first payload from Rio Grande, Brazil, a quite similar breakdown problem occurred during flight and the second payload was not launched.

Following the troubles at Brazil, the second Wallops payload has been subjected to considerable further testing and it is now believed that all problems related to high voltage breakdown have been resolved.

The principle problem is related to the conversion of 28.5 volts to 1800 volts and the leads to carry the 1800 volts to the multiplier compartment. Breakdown was observed interior to the commercially produced converter and, although verification has not yet been obtained, it would seem that the connectors used and the interconnection wiring would both have the same problem.

The problem essentially is that the pumping speed of the electronics packages, the converter in particular, is quite slow and thus the interior pressure does not drop sufficiently below the minimum of the Paschen curve to prevent the breakdown from occurring. The package operates normally at atmospheric pressure and also at the ambient pressures encountered during flight if maintained at these pressures for an extended period of time to allow the slow pumping speed to carry the interior pressure to ambient.

III. WORK IN PROGRESS

The high voltage breakdown difficulties are being resolved by sealing all of the high voltage circuitry and wiring and maintaining this package at atmospheric pressure throughout the flight. This requires almost complete rearrangement of the electronics but this alteration is finished on the Wallops payload and testing is currently being conducted.

As soon as the Brazil payload reaches the laboratory the modifications will be made on it and further tests conducted. This payload is tentatively scheduled for a launch on a Nike-Cajun vehicle from Wallops Island on May 16, 1967.

Plans for the Wallops package will be formulated following the May 16, 1967, launch. Some modifications of the quadrupole and multiplier compartments remain to be done on this package however.

Preliminary efforts are also being made toward the development of a negative ion mass spectrometer for use in ionospheric research.

APPENDIX

CHAPTER AI

INTRODUCTION

The quadrupole mass filter is a recently introduced device which transmits only ions of a fixed charge-to-mass (e/m) ratio. By changing its electrical parameters it is possible to change the charge-to-mass ratio of ions which will be transmitted. Thus, a wide range of ions can be investigated in succession.

The theory of the quadrupole mass spectrometer was developed in 1955 by Dr. Wolfgang Paul and others at the University of Bonn from extensive earlier work on strong focusing electric and magnetic lens systems. Since then, several types of quadrupole filters have been used for detection of ions in different mediums.

The apparatus is particularly well suited for upper atmosphere research because it combines high sensitivity with small size and low power requirements. Recently (1965, Narcisi and Bailey) it was used at heights between 60 - 120 km and interesting results were obtained. Light metallic ions appeared between 95 and 110 km and their distribution suggested that the night-time E-region ionosphere is maintained by ionized metal atoms but this still requires further study.

This work discusses the electronic equipment of the mass spectrometer for ionospheric investigations. The equipment is designed to suit particularly the mass range of light metals and atmospheric gases. The low (less than 8 amu) and high (greater than 50 amu) mass ranges are not covered.

Wherever possible, miniature components are used because the apparatus was to be put in a limited space in a rocket. Solid state devices are used for most active components.

Standard techniques of encapsulating all the components are applied in order to ensure rigidity and protection against acceleration and shocks.

The apparatus was tested and calibrated under normal conditions, which differ from expected working conditions.

CHAPTER AII

MASS SPECTROMETRY

Introduction

The mass spectrometer has an e/m band pass characteristic for charged particles. It is obtained by applying a high frequency field on four hyperbolic electrodes (Fig. 1). With the applied voltages of opposite sign on the y and x hyperbolas the potential between electrodes is :

$$\Psi = V(t)\frac{(x^2 - y^2)}{r_o^2} \qquad 1.1$$

where $r_o^2 = x_o^2 - y_o^2$

and the electric field is

$$E = -2V(t)(x\hat{x} - y\hat{y}) \qquad 1.2$$

The equation of motion of a charged particle with mass m and charge e in such a field is

$$m\frac{d^2r}{dt^2} - eE = 0 \qquad 1.3$$

which is equivalent to:

$$m\frac{d^2x}{dt^2} + eV(t)\frac{x}{r_o} = 0 \qquad 1.4$$

$$m\frac{d^2y}{dt^2} - eV(t)\frac{y}{r_o} = 0 \qquad 1.5$$

$$m\frac{d^2z}{dt^2} = 0 \qquad 1.6$$

Equation 1.6 shows that the velocity of a particle is constant along the z direction.

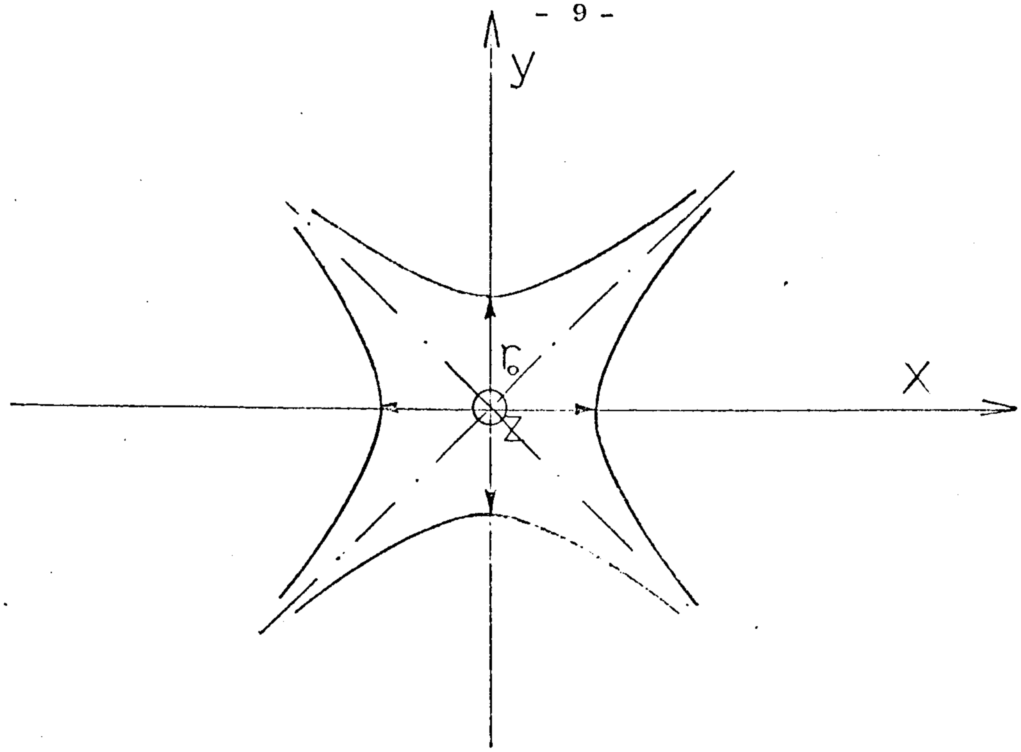

Figure 1
Hyperbolic Electrodes

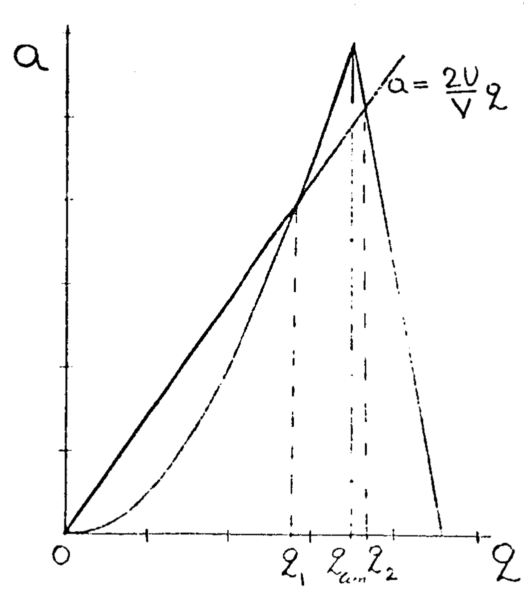

Figure 2
Stability Diagram (Vertical .04 per division, Horizontal .2 per division)

For $V(t) = U + V\cos(\omega t)$ and with a change of variable $\omega t/2 = \xi$, equations 1.4 and 1.5 become:

$$\frac{d^2x}{d\xi^2} + (a + 2q\cos 2\xi)x = 0 \qquad 1.7$$

$$\frac{d^2y}{d\xi^2} - (a + 2q\cos 2\xi)y = 0 \qquad 1.8$$

where:

$$a = \frac{8eU}{m r_0^2 \omega^2} \qquad q = \frac{4eV}{m r_0^2 \omega^2} \qquad 1.9$$

Equations 1.7 and 1.8 are the normal form of Mathieu equations for which the solution is of the form:

$$x = \alpha_1 e^{\mu\xi} \sum_{-\infty}^{\infty} C_{1s} e^{-2is\xi} + \alpha_2 e^{-\mu\xi} \sum_{-\infty}^{\infty} C_{2s} e^{-2is\xi} \qquad 1.10$$

The initial entrance conditions of ions are contained in α_1, α_2, C_{1s}, and C_{2s}, and u depends on a and q.

Stable oscillations in the x direction are obtained for those $u(a_x, q_x)$ for which $x < \infty$ when $\xi \to \infty$. The same is true for the y direction. The range of a_x, q_x corresponding to stable oscillation in the x direction can be plotted in the a_x, q_x plane. The same applies for a_y, q_y. Since $a_x = -a_y$ and $q_x = q_y$, we see that the overlapping mirror image of stable a_y, q_y about the q axis, with stable a_x, q_x, will give the stable region for both components of oscillation.

For the fixed field and dimension specifications r_o, ω, U, and V, all ions of identical mass have the same operating point a, q. If the point lies within the three-sided region in the a, q plane (Fig. 2), stable and undamped oscillation in the x-y plane will result. On the edge of the region the oscillations are undamped. Outside the region the amplitude of oscillation rapidly increases.

The ratio $a/q = 2U/V$ is independent of the mass and therefore all ions of different masses lie on a straight line $a = 2U/V\ q$ in the stability diagram (Fig. 2). Only those ions whose operating point satisfies $q_1 < q < q_2$ will be stable. By increasing the U/V ratio the stable q interval (which corresponds to stable mass interval) becomes smaller until it reaches the point $q_1 = q_2 = q_{lim} = .706$ with corresponding $a_{lim} = .236$ and $U/V = .167$. When the intersection of line $a = 2U/V\ q$ with the three-sided stability curve approaches the point (a_{lim}, q_{lim}) only ions of one definite mass will have a stable path, while all the others will have unstable oscillations and will end on the electrodes. (It also may happen that ions with stable paths end on electrodes because of a large starting amplitude.)

For fixed U/V ratio there will be a possible mass interval m_1, m_2 corresponding to q_1, q_2. (In practice this mass interval should not contain more than one distinct mass.)

In practice mass resolving power is defined using the voltage at the output of electron multiplier as the mass spectral line is scanned. It is the ratio of the mass number of the spectral line to the width of the spectral line at 10% of its peak expressed in mass number units.

For a desired resolving power, parameters a and q have to be stabilized to better than $\Delta m/2m$ of their values. Hence it follows that the D.C. voltage U and the high frequency voltage V must be stabilized to better than $\Delta m/2m$ and the frequency f and radius r_o must be constant to better than $\Delta m/4m$.

If one wants to sweep a range of ions it is possible either to keep the frequency constant and vary V with the U/V ratio constant or to vary the frequency keeping U and V constant.

Mass Spectrometer and Electrical Components:

In Fig. 3 is shown a diagram of the actual mass spectrometer for ionospheric investigation.

The cylindrical rods with $r = 1.16\ r_o$ are a good approximation to hyperbolical rods and can be easily made. In front of the rods are two focusing electrodes at potentials $-V_1$ and $-V_2$, $(V_2 > V_1)$. At the end stands an exit aperture with the hole on the axis leading to the electron multiplier.

The ions which have a component of velocity parallel to the rods after being focused start to oscillate between rods. The stable ones hit the cathode of the electron multiplier (through aperture). Secondary electrons are emitted from the cathode and a multiplication process starts which leads to a burst of electrons which hits the anode of the multiplier. This current serves as the input to the log amplifier.

If the component of the velocity of ions parallel to the rods is v the number of oscillations along the rods for an ion is simply:

$$n = \frac{L}{v} f \qquad 1.11$$

and it should be relatively large so that the stable ions have enough oscillations to get well resolved from the unstable ions.

In the actual experiment the relative velocity of ions with respect to the rods (and parallel to the rods) will be near the velocity of the rocket.

If frequency modulation is used for sweeping the mass range all the

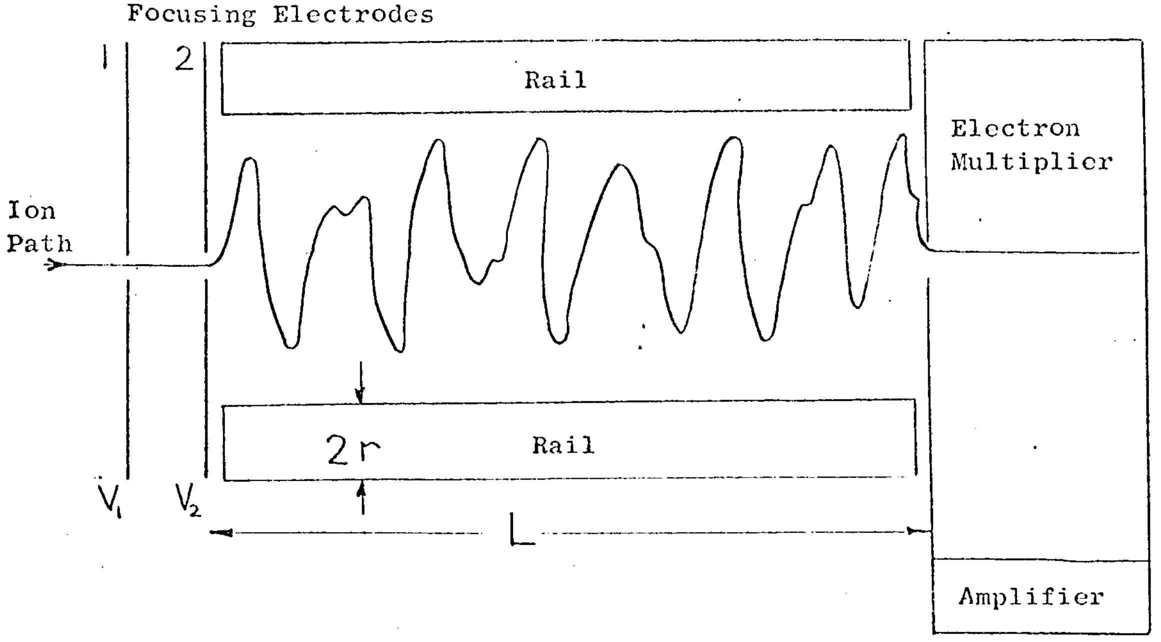

Figure 3
Mass Spectrometer

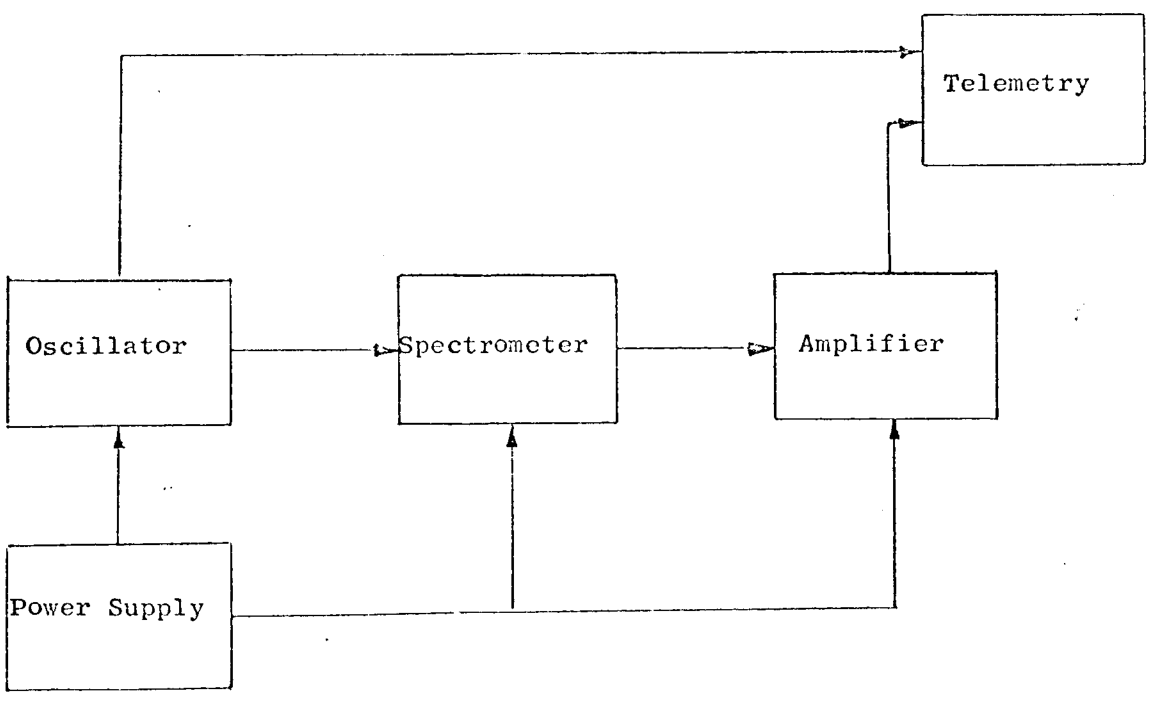

Figure 4
Block diagram of electrical components

ions will not have the same resolution as n depends on the frequency. However if the frequency is high the difference in resolution between lower and higher mass numbers will be negligible. The resolution will be better than in the case of amplitude modulation because the constant ratio in amplitude modulation is more difficult to obtain due to variation of V.

The block diagram of electrical components in Fig. 4 consists of power supply, oscillator, electron multiplier, amplifier, and telemetry systems. The available space in the rocket was the dominant factor for the choice of solid state devices for all components (except an electrometer tube used in the log amplifier). Their low power consumption and inherent rigidity were other advantages over tubes. Again because of limited space and less complicated circuitry an amplitude modulated oscillator has been chosen. The apparatus had to meet the following mechanical specifications:

1. Vibration

   a) ± 1/4 inch double amplitude from 5 to 25 cps.

   b) 5 g acceleration from 25 to 2000 cps sweep 1 minute per octave

2. Shock

   100 g shock 11 ms total duration and half-sine pulse form

3. Acceleration

   50 g steady acceleration along longitudinal axis for 30 seconds

4. Spin

   12 rps spin about longitudinal axis 6 minutes

CHAPTER AIII

ELECTRICAL COMPONENTS

The amplitude modulated driving oscillator consists of three main parts (Fig. 5): the sweeping circuit, the oscillator, and the rectifier with adding circuits. It had to meet the following requirements:

1. To provide sufficient amplitude and frequency in order to cover the mass range from 10 amu to 50 amu.

2. To sweep the chosen mass range once every 1/2 second so that samples of ions could be taken every 1/2 Km (the speed of rocket = 1Km/s).

3. Rectified and attenuated sweep from the output of the oscillator had to be transmitted through a telemetry system. That was the only data for timing the results which were also to be transmitted by telemetry. In the same time the sweep could be used for checking the oscillator at work. The telemetry system could accept a signal with a voltage range from 0 to 5 volts.

For $q = q_{Lim}$ and $a = a_{Lim}$ the following relation (from Eq. 1.9) between parameters is easily obtained:

$$V_{(volts)} = 7.21\, f^2_{(MC)}\, r_{o\,(cm)}^2\, A \tag{2.1}$$

where A is the mass number.

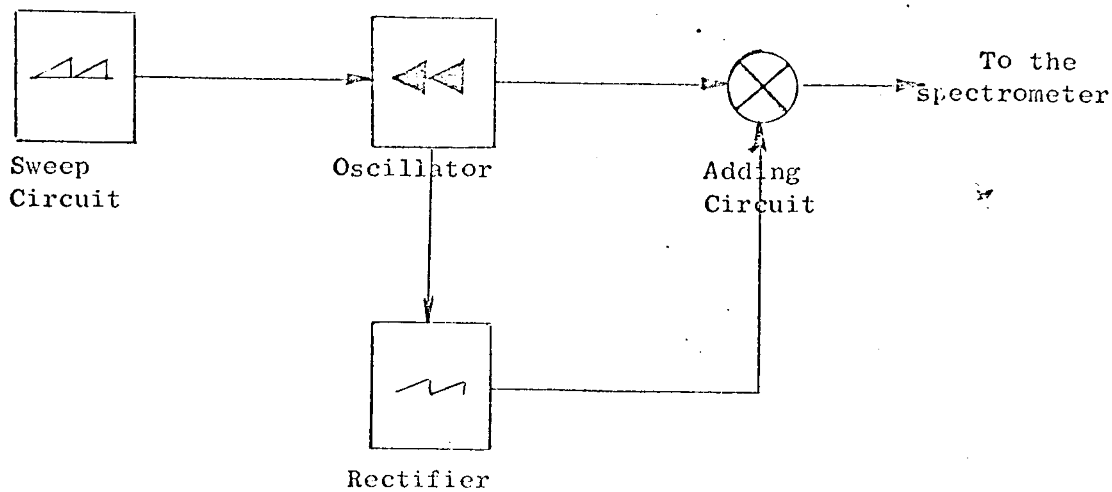

Figure 5
Driving Oscillator--block diagram

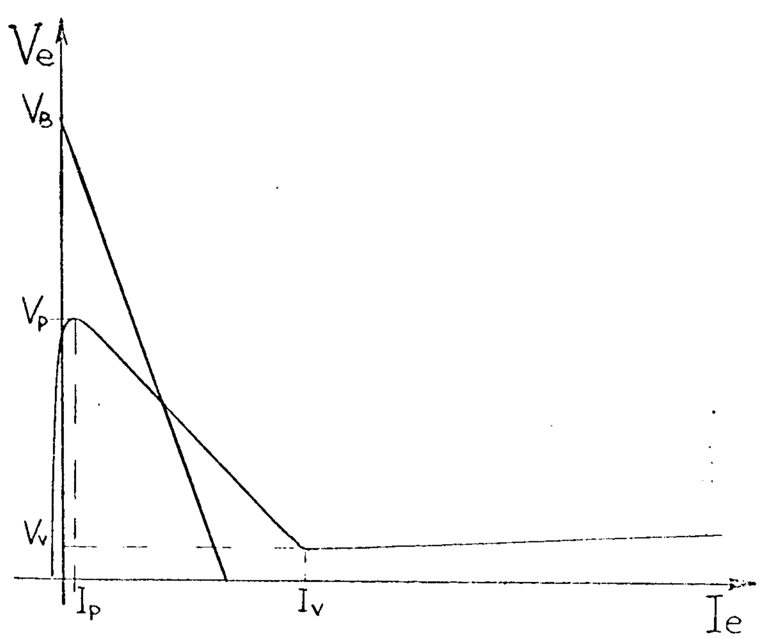

Figure 6
Load line in $I_e V_e$ characteristics

Since the mass spectrometer represents essentially a capacitance load, the power developed in the equivalent output tank circuit is:

$$P = \frac{4V^2 C_e \pi f}{Q} \qquad 2.2$$

where C_e is the equivalent capacity and Q is the equivalent Q factor of the tank circuit.

The peak A.C. voltage V which we considered realizable was $V = 300v$ and with the dimensions of the spectrometer ($L = 4''$, $2r = .25''$) and speed of the rocket: $v = 1 Km/s$ the frequency needed to reach $A = 50 amu$ becomes $f = 3.3 MC$

The number of oscillations of an ion is $n = 600$. That is the average number of oscillations in the entire range and it is sufficient for good resolution provided that the oscillator output is symmetrical.

<u>Sweep Circuit:</u>

Since a linear sweep was not essential, it was possible to use a standard unijunction-transistor sweep circuit (Fig. 7). In order not to exceed the base to base voltage (V_{BBmax}) limit, the base B_2 is returned through a divider $R_1 R_2$ to the power supply V_B. This arrangment also improves the linearity of the sweep because the capacitor is charging toward a much larger voltage than the triggering voltage V_P. V_P is directly proportional to the interbase voltage V_{BB} intinsic standoff ratio η and forward emitter base voltage V_D :

$$V_P = V_{BB}\eta + V_D \qquad 2.3$$

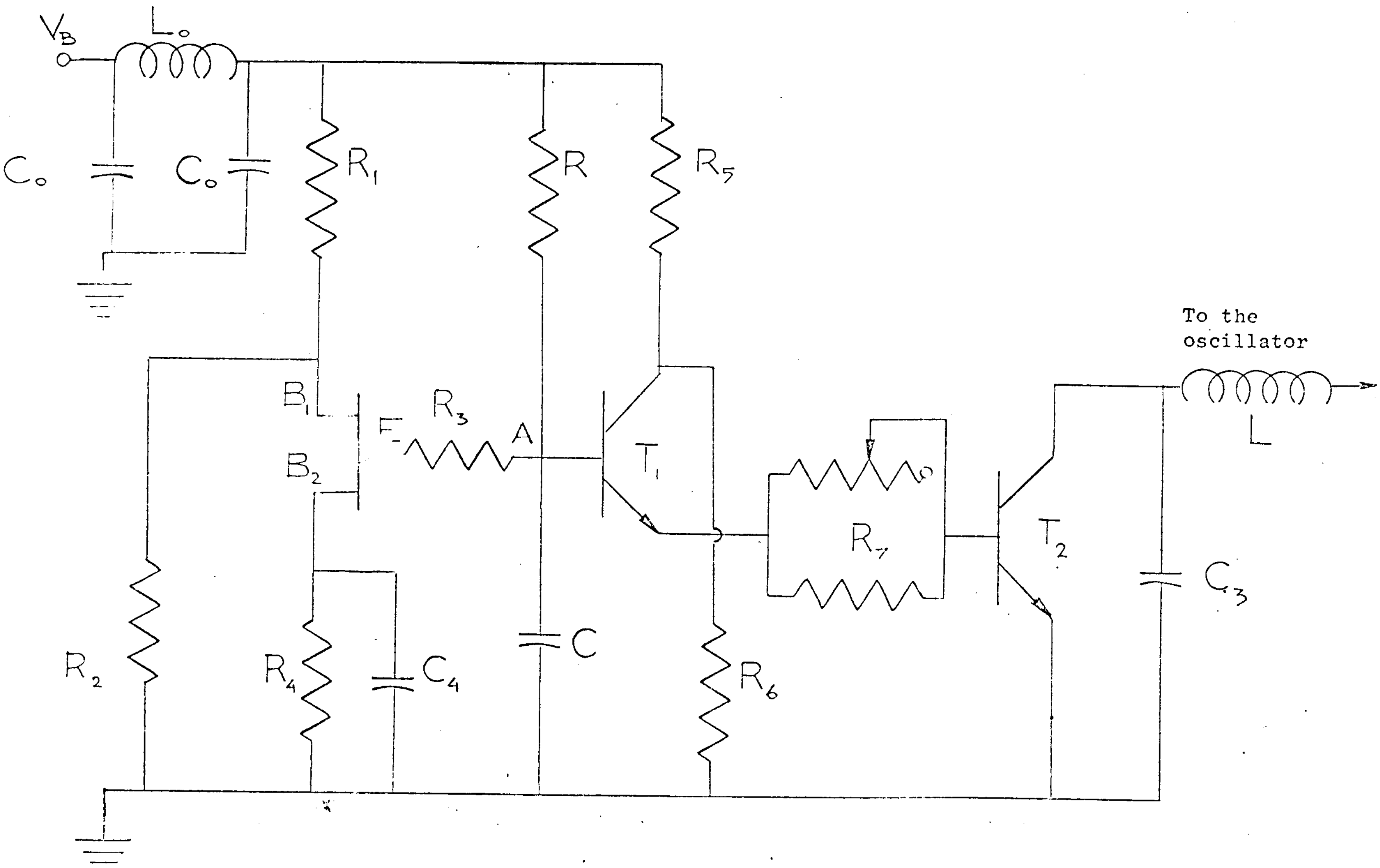

Figure 7
Sweep circuit and decoupling circuit with driving transistor

Because of the variation of interbase resistance R_{BB} for different transistors there will be a range of possible V_{BB}:

$$V_{BB_{min}} = \frac{V_B}{R_1 + \frac{R_{BB_{max}} R_2}{R_{BB_{max}} + R_2}} \cdot \frac{R_{BB_{max}} R_2}{R_{BB_{max}} + R_2} \qquad 2.4$$

and:

$$V_{BB_{max}} = \frac{V_B}{R_1 + \frac{R_{BB_{min}} R_2}{R_{BB_{min}} + R_2}} \cdot \frac{R_{BB_{min}} R_2}{R_{BB_{min}} + R_2} \qquad 2.5$$

For this range of V_{BB} from static unijunction characteristics, or using Eq. 2.3, V_P can be found.

The estimate of RC (time constant which generates the time base) can be found assuming that V_C rises linearly. The approximation is very close because of the small portion of the supply voltage to which C is charged:

$$V_C = V_B\left(1 - e^{-\frac{t}{CR}}\right) \approx V_B \frac{t}{CR} \qquad 2.6$$

At $t = T_S$, where T_S is the sweep period, $V_C = V_P$. Thus

$$CR = \frac{V_B T_S}{V_P} \qquad 2.7$$

The resistance R must be chosen in such a way that the intersection of the load line with the $V_e I_e$ characteristic lies in the region where the slope dV_e/dI_e is negative (Fig. 6).

Thus:

$$\frac{V_B - V_P}{I_P} > R \qquad 2.8$$

$$\frac{V_B - V_V}{I_V} < R \qquad 2.9$$

However the particular R in this range has to be chosen experimentally in order to achieve exactly a time base T_S, because of the normal variations of η and R_{BB} between unijunction transistors.

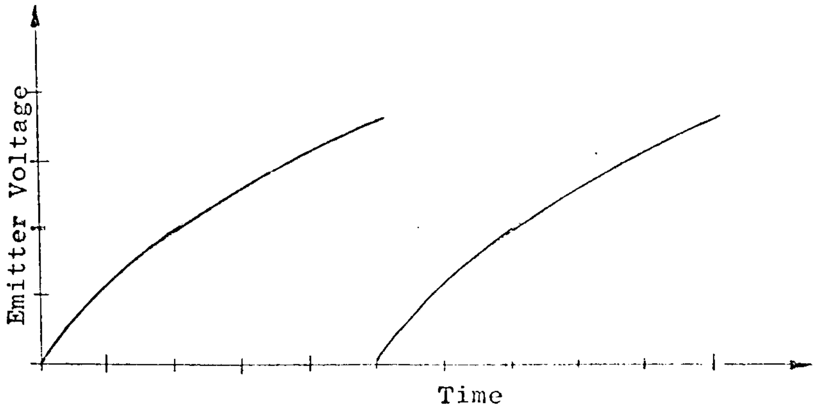

Figure 8
The sweep at the emitter
Vertical 2V/cm Horizontal .1 S/cm

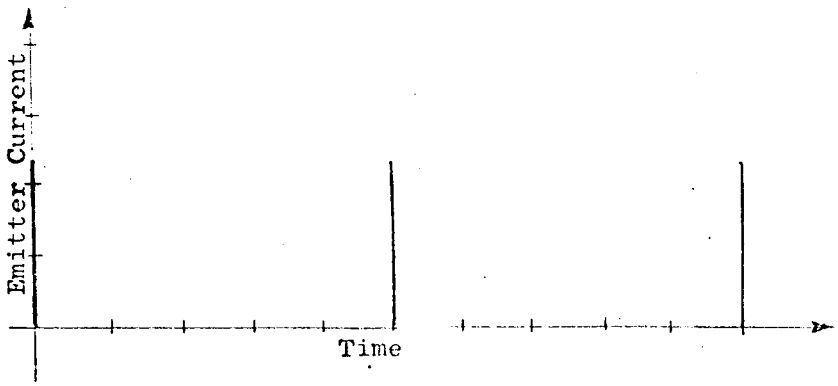

Figure 9
Peak current through the junction
Vertical 42 mA/cm Horizontal .1 S/cm

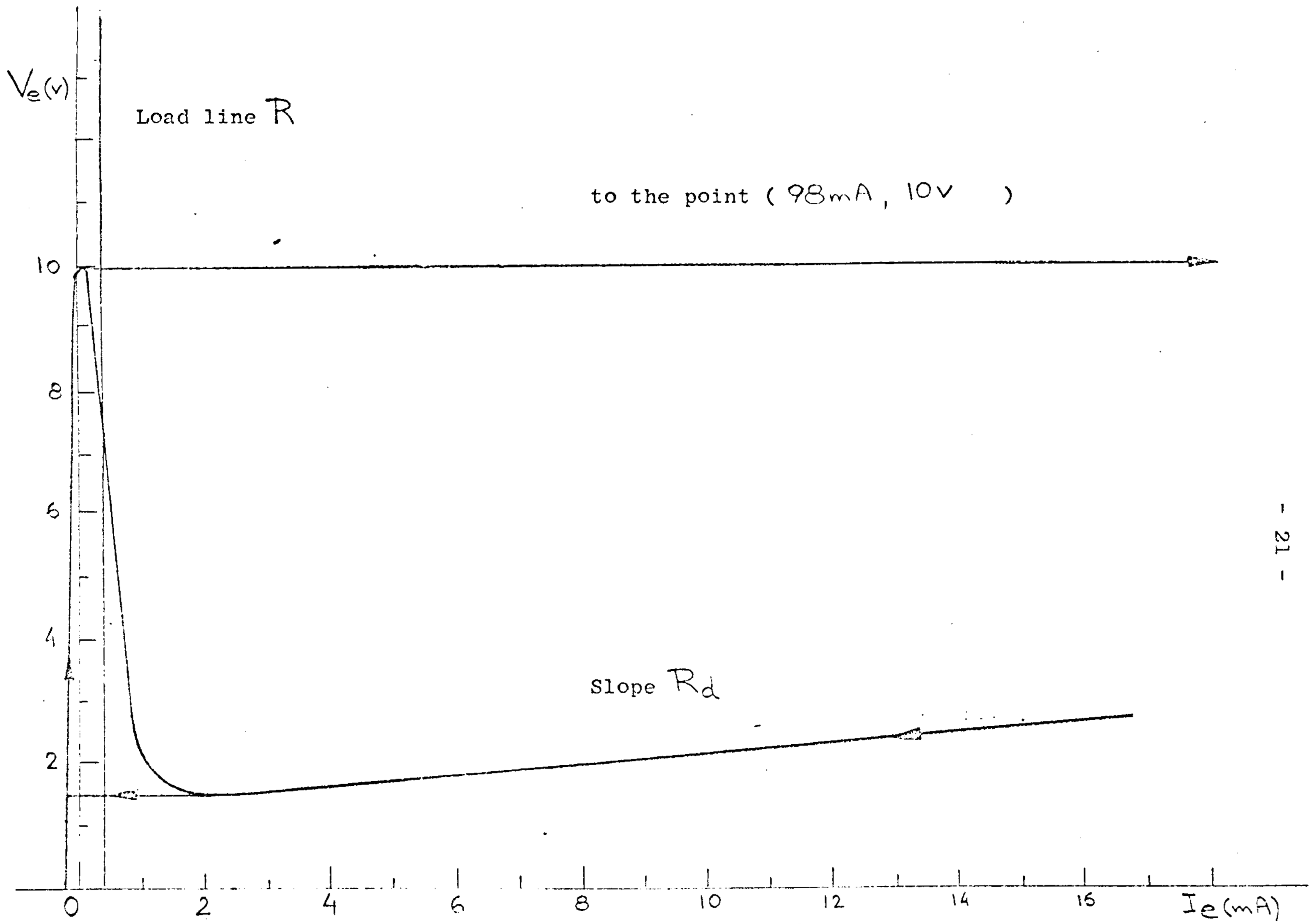

Figure 10
Operating path of unijunction transistor

Resistors R_3 and R_4 protect the junction from high current during the transient in triggering. Capacitance C_4 compensates for the capacitance between the emitter and base number two.

The actual operating path of a unijunction transistor is shown in Fig. 10. It is an approximation to the real conditions in the circuit because the small lead inductance is ignored. The time constant during turn off time is simply

$$\tau = C\,(R_3 + R_4 + R_d) \tag{2.10}$$

and has to be less than 5% of the sweep period.

<u>Decoupling Circuit</u>:

This circuit consists of an emitter follower T_1. The collector is returned to the supply voltage V_B through the divider $R_5 R_6$ (Fig. 7) so that its voltage never exceeds the permitted range:

$$\frac{R_6}{R_5 + R_6} V_B < V_{CB_0} \tag{2.11}$$

In order not to prevent relaxation oscillation the voltage at its base (when the circuit is disconnected at point A) must be larger than the firing voltage V_P :

$$\frac{V_B R_7 (h_{FE_1} + 1)}{R + (h_{FE_1} + 1) R_7} > \frac{\dfrac{V_B R_2}{R_1 + R_2} (\eta R_{BB} + R_4)}{\dfrac{R_1 R_2}{R_1 + R_2} + R_{BB} + R_4} \tag{2.12}$$

this gives:

$$\frac{R_2 (\eta R_{BB} + R_4)}{R_1 R_2 + (R_{BB} + R_4)(R_1 + R_2)} < \frac{(h_{FE_1} + 1) R_7}{R + (h_{FE_1} + 1) R_7} \tag{2.13}$$

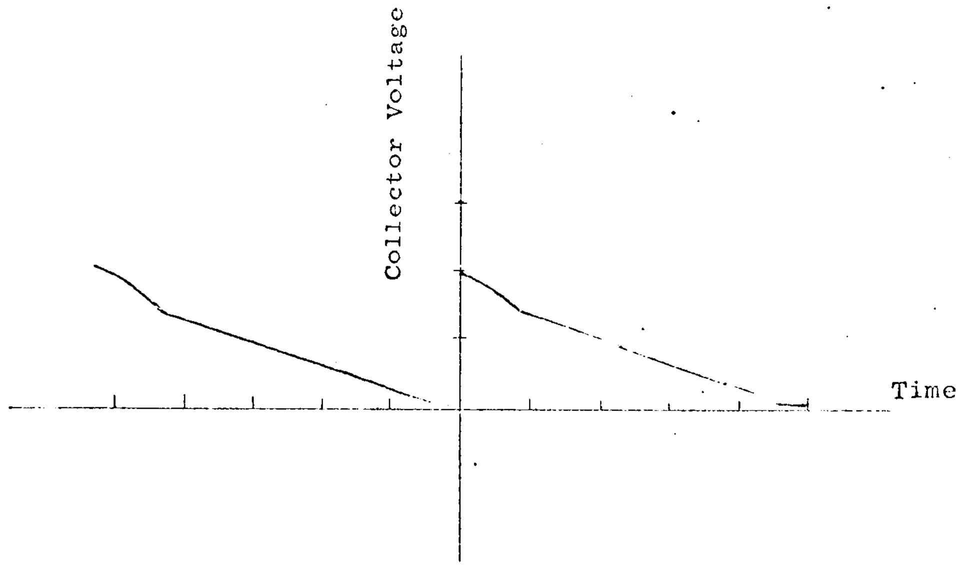

Figure 11
Collector voltage of the driving transistor
Vertical 50V/cm Horizontal .1S/cm

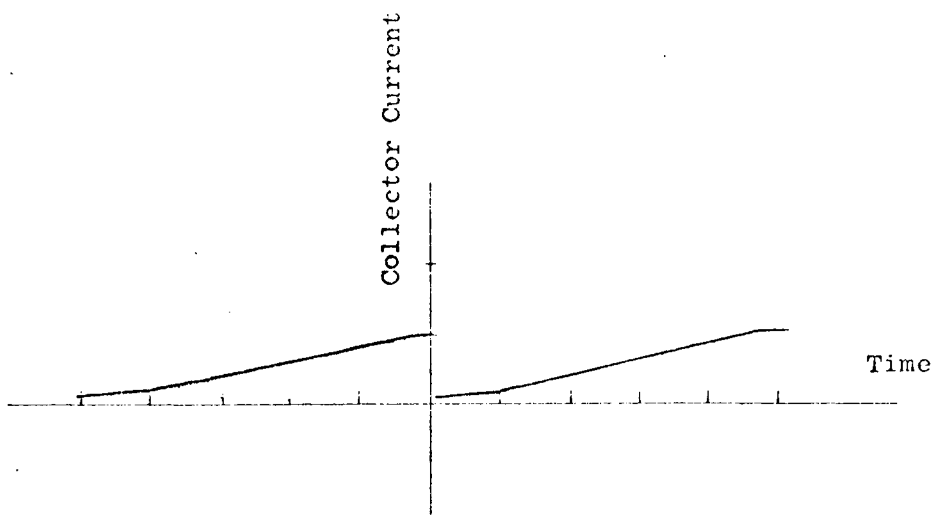

Figure 12
Collector current of driving transistor
Vertical 100mA/cm Horizontal .1S/cm

To prevent saturation when the sweep reaches its peak R_5, R_6, and R_7 must satisfy the following condition:

$$\frac{V_B R_6}{R_5+R_6} - \frac{R_6 R_5}{R_6+R_5} \cdot \frac{V_P\, h_{FE_1}}{(R_7+h_{ie_2})(1+h_{FE_1})} > V_P \qquad 2.14$$

R_7 consists of a potentiometer in parallel with fixed resistor so that the base current of the driving transistor T_2 can be adjusted so that at V_P transistor T_2 takes the maximum current I_{max} (sufficient to give the necessary voltage for the maximum mass number). Thus

$$\frac{V_P}{R_7} h_{FE_2} = I_{max}$$

T_2 must be a power transistor with audio frequency response sufficient to follow the retrace time of the sweep. The maximum swing of collector voltage is V_B which is also the maximum applied to the collector base junction.

Power dissipated in the transistor can be found if the actual waveforms of the collector current and voltage (Fig. 11-12) are replaced by a linear approximation. Therefore:

$$V_{ce} = V_B - \frac{V_B - V_{min}}{T_S} \cdot t \qquad I_c = I_{min} + \frac{I_{max} - I_{min}}{T_S} t \qquad 2.15$$

The power dissipation is

$$P = \frac{1}{T_S}\int_0^{T_S} V_{ce} I_c \, dt = \frac{V_B I_{max} + V_{min} I_{min}}{2} - \frac{(V_B - V_{min})(I_{max} - I_{min})}{3} \qquad 2.16$$

In the case $I_{min} \ll I_{max}$ and $V_{min} \ll V_B$ the power is

$$P = \frac{1}{6} I_{max} V_B \qquad 2.17$$

An $L_o C_o$ filter between the driving circuit and the power supply was used because the high frequency oscillator uses the same power supply. Its components must satisfy:

$$L_o \omega \gg \frac{1}{C_o \omega} \qquad 2.18$$

Capacitor C_3 across T_2 is to short circuit the high frequency and its maximum value is determined by the fact that it must follow the turn off time of the sweep while discharging through T_2.

High Frequency Oscillator:

This oscillator is a push-pull type with two coupled tanks in series (Fig. 13). Push-pull is chosen to give the equal and opposite voltages necessary for the spectrometer rods. An auto transformer connection gives the large voltage V which otherwise could not be obtained because of the V_{cbo} limitation of the transistors.

Transistors T_3 and T_4 are alternately in saturation and thus act like switches inserting energy alternately to each half of the coil. By means of the $R_1 C_1$ network between collector and base of the opposite transistors, a closed loop and positive feedback are obtained. In order to have the gain greater than one h_{FE} must be greater than one at the oscillation frequency. The time constant $R_1 C_1$ must be of the order of $3T$ to $5T$ (where T is the period of oscillation), so that the base of the non-conducting transistor is maintained negative during approximately $1/2\,T$. The capacitor charges during the on time through the power supply (V_b, I_b), coil L_1, and emitter base of the on transistor. The time constant in charging the capacitor must be much smaller than T : $C_1 h_{ie} \ll T$

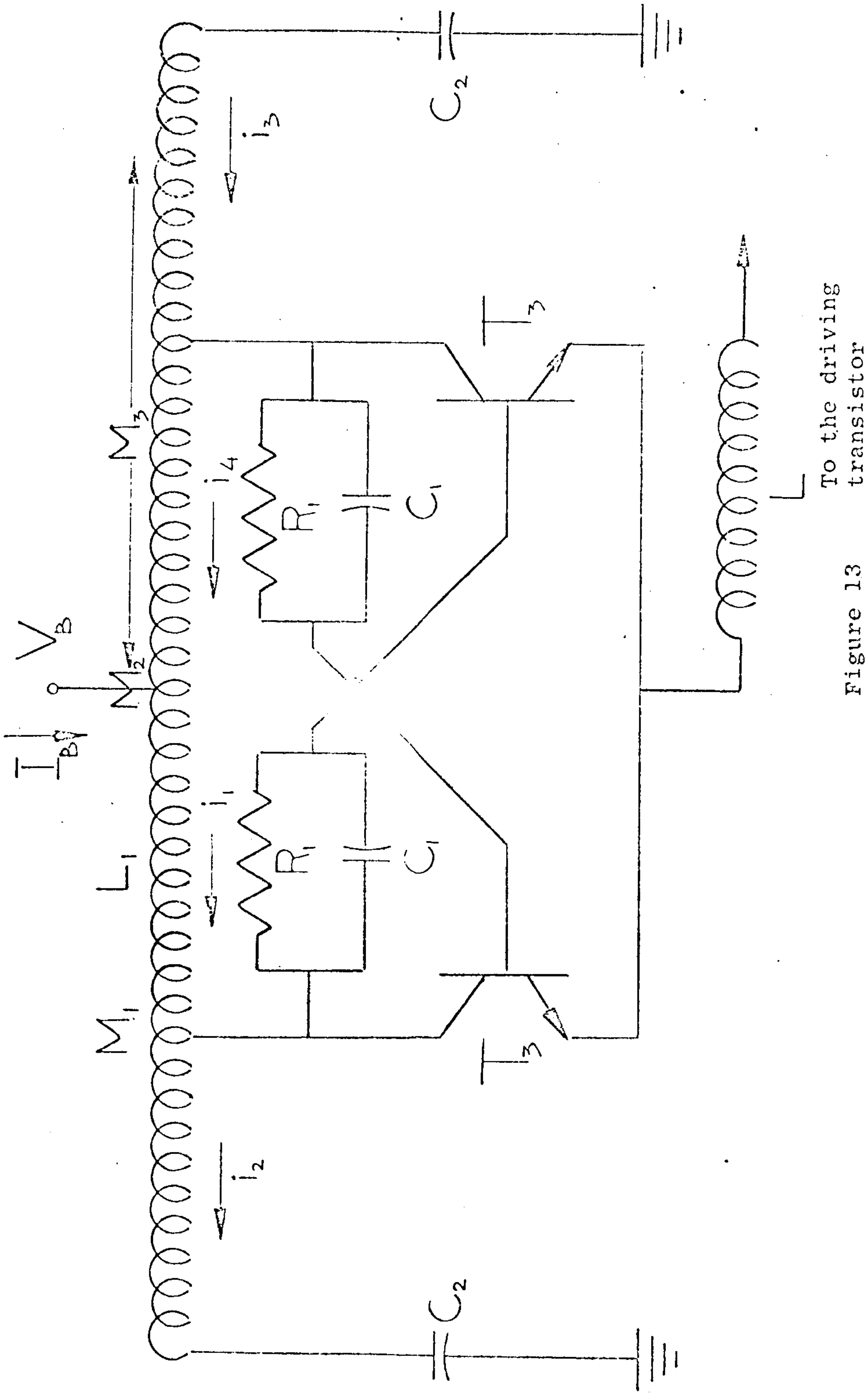

Figure 13
Oscillator

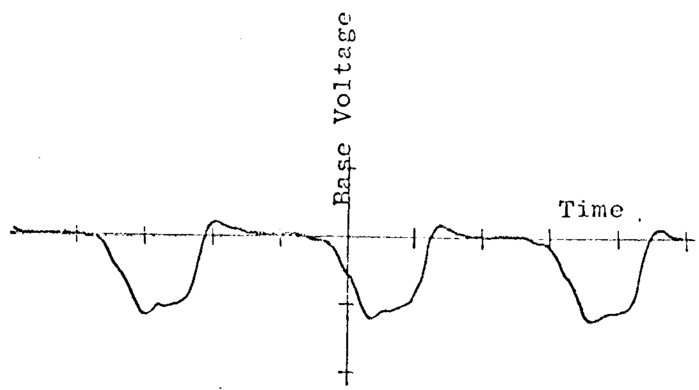

Figure 14
Base emitter voltage
Vertical 10V/cm Horizontal .1 μs/cm
with (I_B=100mA, V_B= 100V)

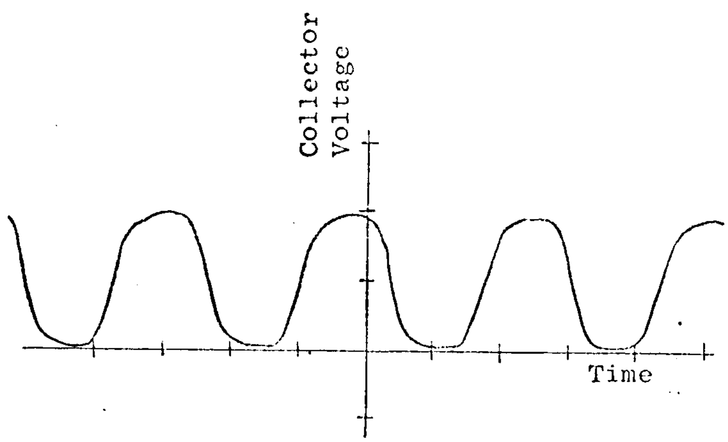

Figure 15
Collector to ground voltage
Vertical 50V/cm Horizontal .1 μs/cm
with (I_b=100mA, V_b=100V)

Figure 14 represents the base emitter voltage. The almost vertical parts of the waveform correspond to transients while zero of voltage corresponds to saturation. The negative part of the waveform which follows the time constant R_1C_1 (almost vertical part of waveform following saturation) corresponds to the transistor being off. The overshoot before the base reaches zero is due to the charging of the capacitor through h_{1e}. The frequency of oscillation is determined essentially by the LC_e components of the circuit: $2C_e = C_2 + C_r$ where C_r is the capacitance of two opposite spectrometer rods with respect to ground plus stray capacitance in the circuit.

Collector voltage (Fig. 15) changes from 0 (when transistor saturates) to $2V_B$ (when it is off).

The transistor has to withstand more than $2V_B$ reverse bias between collector and because the base is negative with respect to ground when $V_c = 2V_B$.

Since the coupling in the coil is very strong, it is possible to find V in terms of a turn ratio $n = N_2/N_1$. Thus

$$V = nV_B \tag{2.19}$$

The experimental relation between V_B and V for $n = 10/3$ is given on Fig. 16 and agrees with the Eq. 2.19. Figure 17 represents the relation between V_B and I_B (I_B = power supply current). Both curves were obtained by changing V_B without the driving transistor in the circuit. The break point at about $V_B = 25V$ happens when the transistors start to saturate and thus draw more current. That produces a break point in the waveform of the voltage because the oscillator is current driven and the characteristic $V_B - I_B$ is the load for the driving transistor T_2.

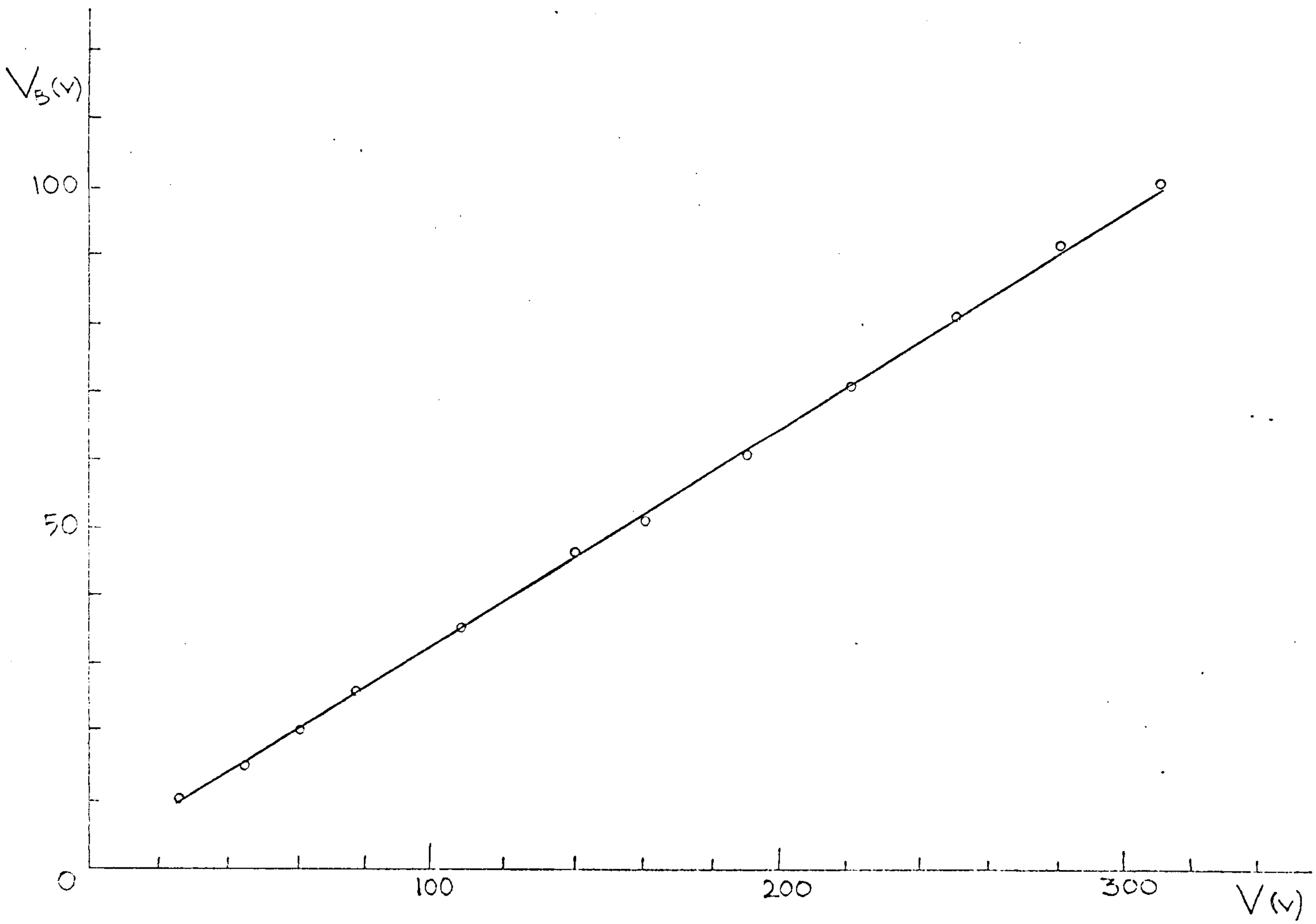

Figure 16
Relation between the D.C. voltage delivered to the oscillator and end of the coil to ground voltage V ($n = 10/3$)

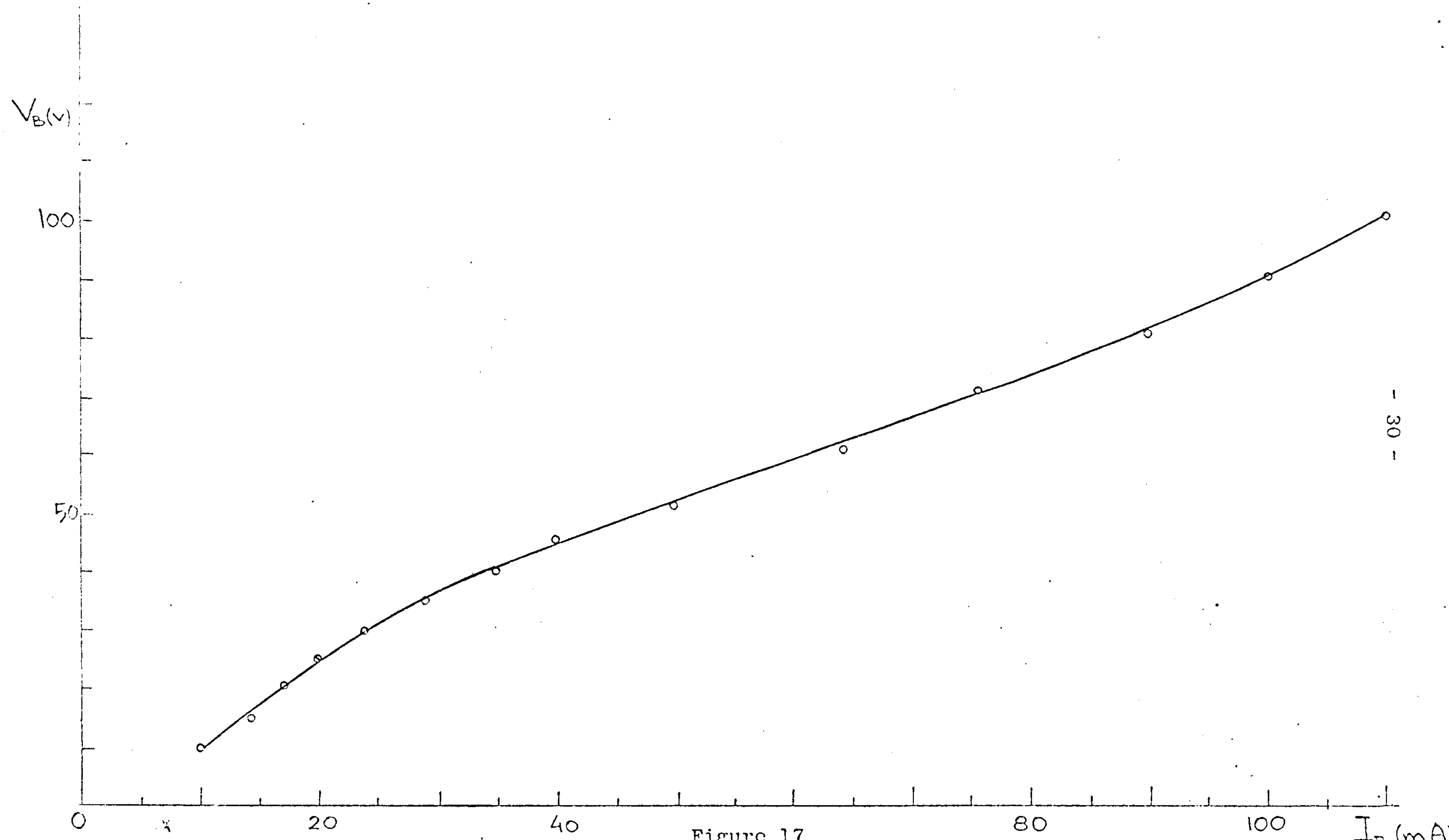

Figure 17
D.C. voltage delivered to oscillator versus supply current

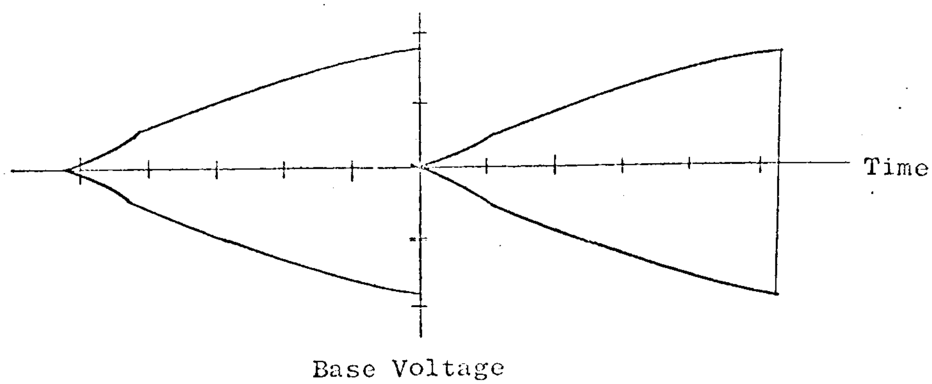

Figure 18
Voltage between the end of the coil and the ground--without L in emitter
Vertical 200V/cm Horizontal .1μs/cm

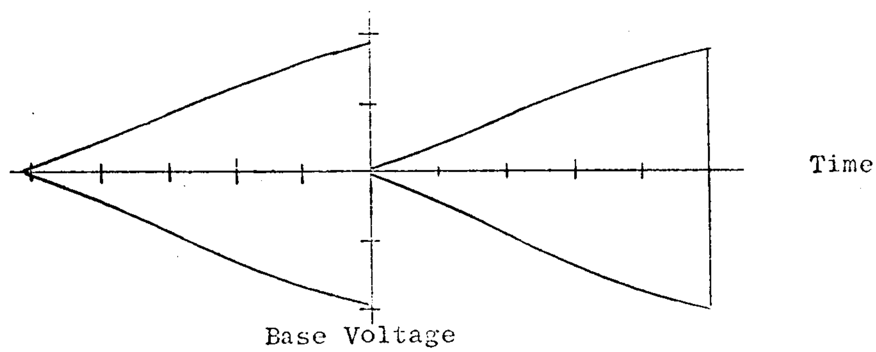

Figure 19
Voltage between the end of the coil and the ground--with L in emitter
Vertical 200V/cm Horizontal .1μs/cm

By using an inductor L in series with the two emitters, it is possible to linearize the waveform of the modulated voltage.

The expression for V_{coe} from (Fig. 13) is

$$V_{coe} = V_B + L_1 \frac{di_1}{dt} + M_1 \frac{di_2}{dt} + M_2 \frac{di_3}{dt} + M_3 \frac{di_4}{dt} \qquad 2.20$$

The current

$$i_2 = n V_B \omega C_2 \cos \omega t$$

is much larger than I_B. Also, $i_2 = i_3 \approx i_1 = i_4$

because the currents through the transistors are small compared to the current in the tank.

With these approximations

$$V_{coe} = V_B + L_e \frac{di_2}{dt} \qquad 2.21$$

$$= V_B + L_e C \omega^2 V_B \sin \omega t$$

where $L_e = L_1 + M_1 + M_2 + M_3$

This expression holds approximately for the values of current near maximum (i.e., for the values of collector voltage $0 < V_{coe} < 2V_B$). The transient time (time during which collector voltage changes from 0 to $2V_B$) is, from 2.21.

$$t_{tr} = \frac{2}{\omega} \arcsin \frac{V_B}{L_e C \omega^2 V_B n} \qquad 2.22$$

The maximum power delivered by the supply is

$$P_{Bmax} = V_B I_{max} \qquad 2.23$$

where I_{max} is the maximum supply current which can be determined experimentally (at the top of the sweep).

The average power delivered by the source is

$$P_B = \frac{1}{T_s} \int_0^{T_s} V_B I_B \, dt = \frac{V_B (I_{min} + I_{max})}{2} \qquad 2.24$$

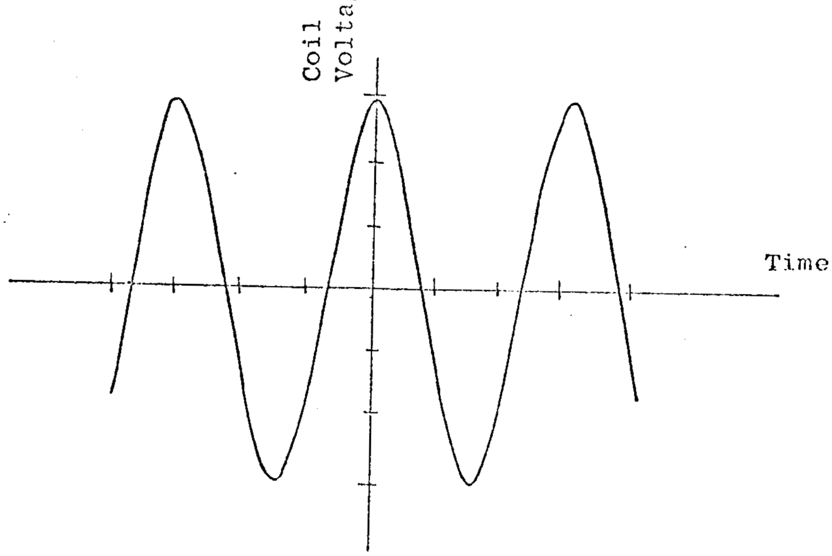

Figure 20
Voltage waveform between end of coil and
ground ($V_B = 100V$ $I_B = 100mA$) without the driver
Vertical 100V/cm Horizontal .1μS/cm

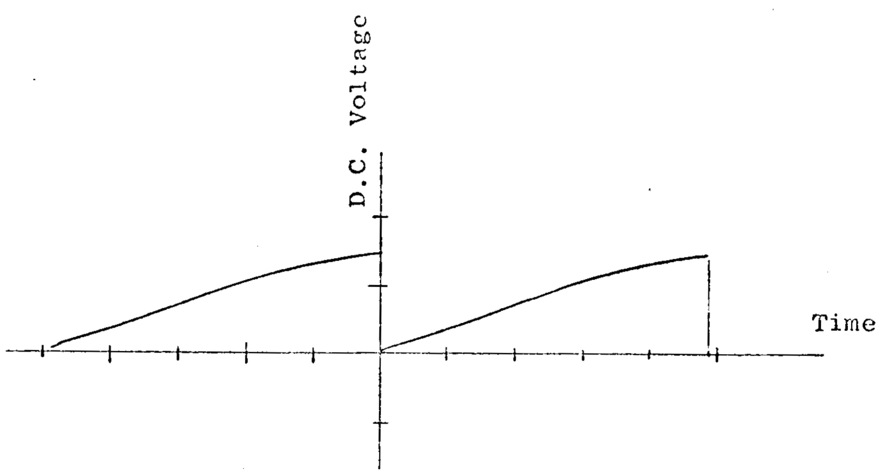

Figure 21
Rectified Sweep
Vertical 50V/cm Horizontal .1 s/cm

since

$$I_B = I_{min} + \frac{I_{max} - I_{min}}{T_s} t$$

The average power dissipated in the coil is:

$$P_{avo} = \frac{1}{T_s} \int_0^{T_s} \frac{4V^2 C e f \pi}{Q} \qquad 2.25$$

where V is the maximum value of the voltage between each end of the coil and ground, given by

$$V = V_1 + \frac{V_2 - V_1}{T_s} t \qquad 2.26$$

The maximum value of V at the beginning of the sweep is V_1 and V_2 is the maximum value of the A.C. voltage at the end of the sweep. With the expression 2.26 for V , P_{avo} becomes

$$P_{avo} = \frac{4 C e \pi f}{Q} \left(\frac{V_2^2 + V_1 V_2 + V_1^2}{3} \right) \qquad 2.27$$

The power dissipation in one transistor is simply

$$P_d = \frac{1}{2} \left(P_B - P_{avo} \right) \qquad 2.28$$

Rectifier and Adding Circuit:

A full wave peak bridge rectifier was used. The bridge is convenient because it represents a symmetrical load to the oscillator. It also reduces the effect of the diode's capacitances. Assuming that the capacitances across the forward and across the reversed biased diodes are of the same order we see that the bridge is nearly balanced with respect to them.

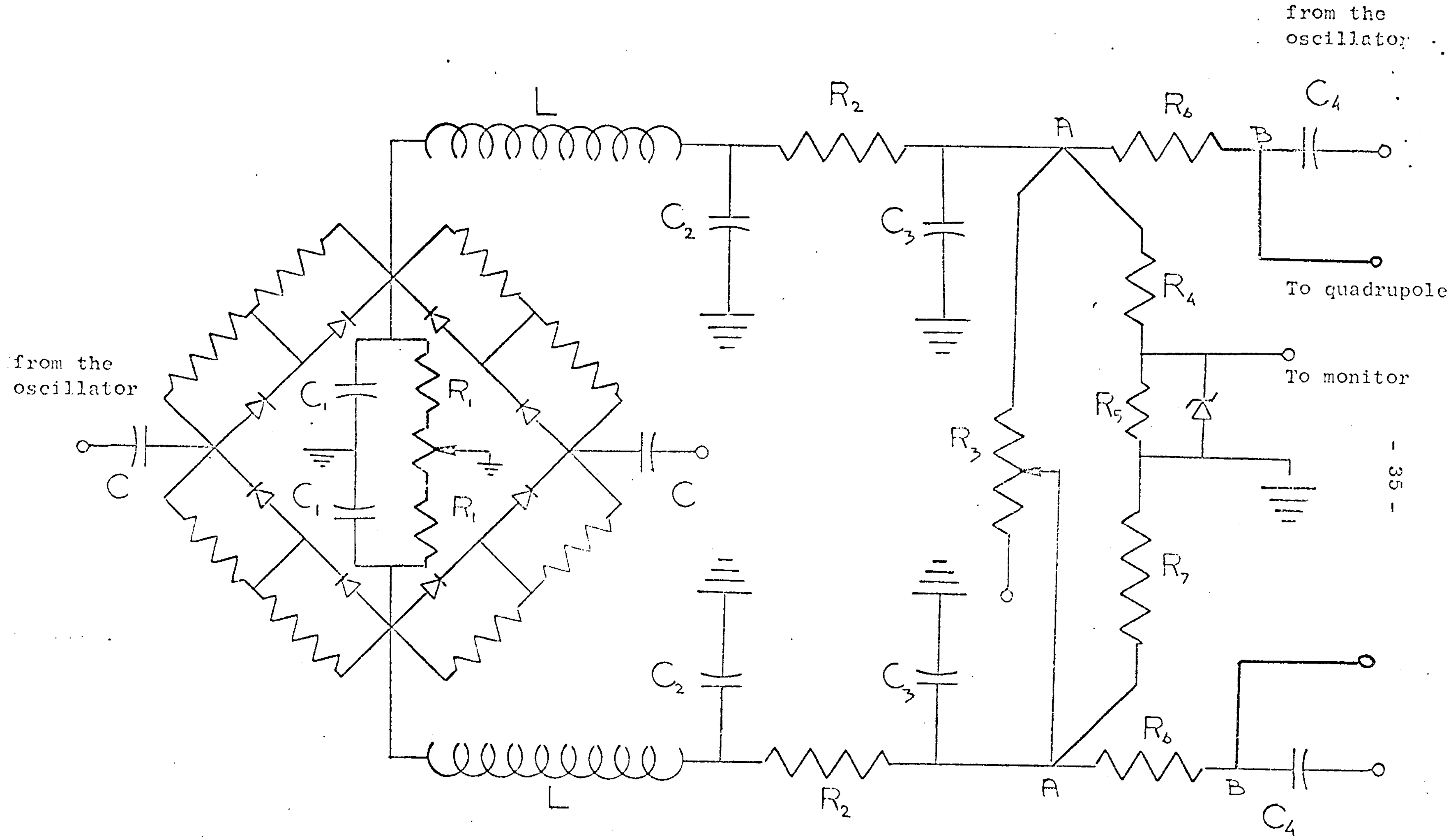

Figure 22
Rectifier and adding circuit

Coming from the oscillator to opposite ends of the bridge are two small coupling capacitors which eliminate the power supply voltage V_B from the rectifier and also reduce the maximum reverse voltage. Two diodes in series are used with a large resistor across each which divides the voltage equally between diodes when they are reverse biased. The diodes in series also reduce the total capacitance in the branch.

The R_1C_1 time constant must be of the order of $5T$ or more so that it can follow the sweep smoothly, while C_1 must be small and of the order of C in order to develop sufficient voltage. A trim potentiometer in series with R_1 balances the D.C. levels with respect to ground.

The D.C. voltage U goes from opposite ends of the bridge through L-C_2-R_2-C_3 to the point B where it adds to the high frequency voltage. L is chosen such that:

$$L\omega \gg \frac{1}{C_2\omega} \qquad 2.29$$

while the time constant $\frac{C_2 C_3}{C_2 + C_3} R_2$ is small compared to the turn off time of the sweep.

At points AA a variable resistance makes it possible to adjust the amplitude of D.C. voltage U. The resistor R_3 is of the order of R_1 and smaller than the parallel resistor leading to telemetry. Thus

$$R_3 \ll \frac{R_5 R_{IN}}{R_5 + R_{IN}} + R_4 \qquad 2.30$$

where R_{IN} is the input resistance of the telemetry amplifier.

Resistor R_7 compensates with respect to ground the effect of R_5 and R_4. Hence

$$R_7 = R_4 + \frac{R_5 R_{IN}}{R_5 + R_{IN}} \qquad 2.31$$

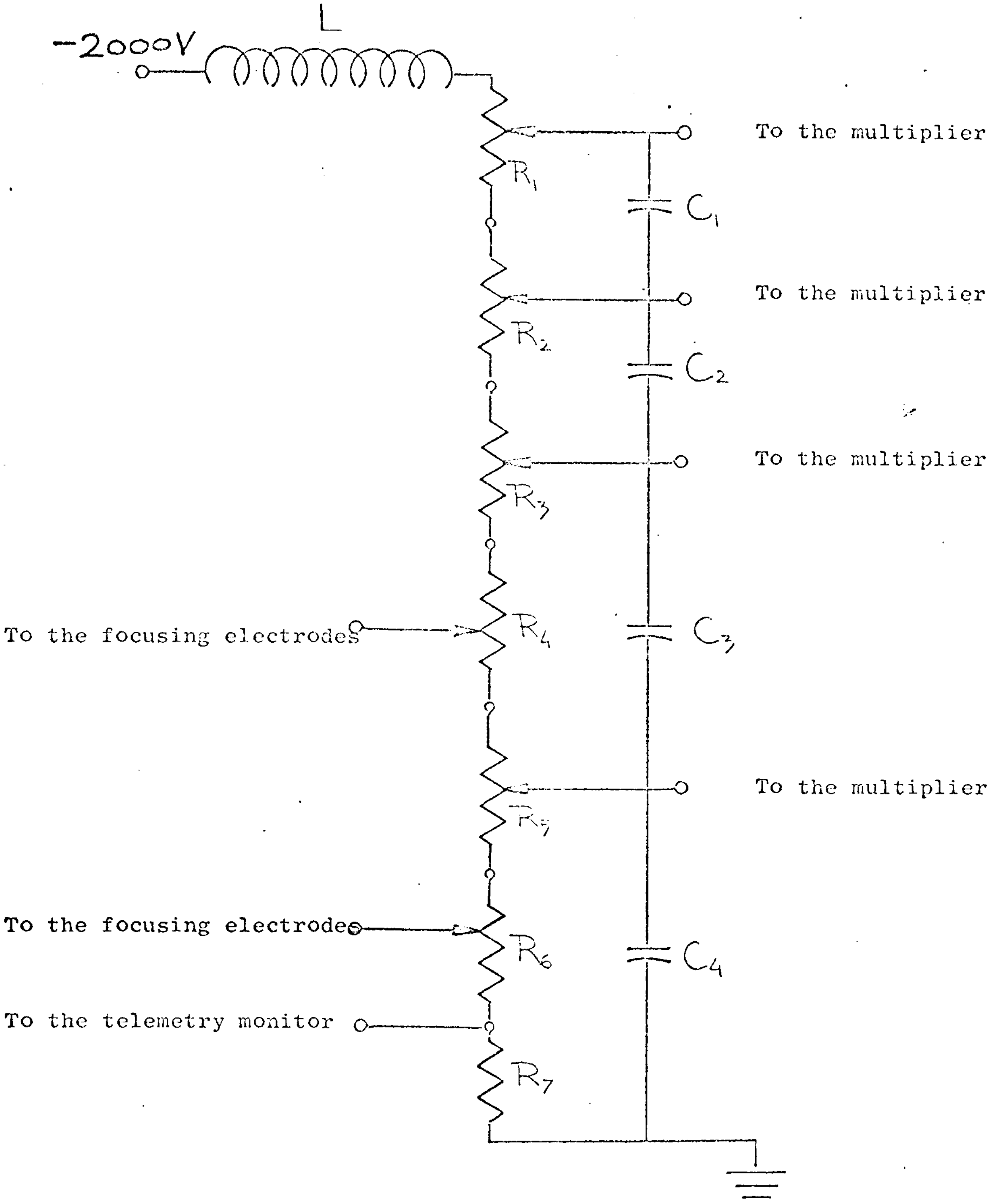

Figure 23
Power Divider

The D.C. voltage is added to the A.C. through a high resistance R_6 so that it does not load the tank.

Power Divider: (Power supply for multiplier, collector, and accelerator)

The output of the power converter is connected to the RC divider (Fig. 23). Choke L in series with RC divider protects the power supply during the transient in turning on. The focusing plates, collector, and telemetry terminals do not need shunting capacitors since variations of voltage at those terminals do not affect the system. The time constant of parallel RC's at the multiplier terminals must be smaller than the period of sweep T_s so that the capacitor is charged in a time less than one cycle of the sweep. It must also be much larger than the time interval between two adjacent masses in order to minimize the effect of voltage peaks produced by ions in the multiplier. Thus the time constant must satisfy

$$\frac{T_s}{A} \ll \tau_{RC} \ll T_s \qquad 2.32$$

where A is the mass range in amu.

Potentiometers provide variable voltages in sufficient range to change the gain of the electron multiplier.

CHAPTER IV

RESULTS AND FURTHER STUDY

Tests and calibrations were carried out under normal conditions with the spectrometer in a vacuum. The spectrometer used to test the electronics was different than the one which will be actually used in the rocket. The primary difference was in the length of rods. The rods used in the test were 5 inches long instead of 4 inches. Because the differences are small the results obtained should not differ significantly from the results expected using the operational spectrometer.

A standard ion source was used to ionize available elements. The ion beam was produced by an electron bombardment source and directed into the mass filter essentially parallel with its axis. Nitrogen, oxygen, and argon were ionized purposely. Water vapor was always present in the vacuum due to imperfection of the system. Conclusions drawn from measurements with those three elements apply with certainty for the mass range from 18 - 40 amu. Outside that range they are a fair guess.

The estimate of mass range is from 8 - 58 amu. **On Fig. 25 are** shown the peaks of nitrogen N_1^+, water H_2O^+, nitrogen N_2^+, oxygen O_2^+ and argon Ar_1^+. We see that the resolution for lower mass numbers 14 and 18 is worse than the resolution for higher mass numbers. That is due to the fact that lower mass numbers have fewer oscillations along the rods because they get higher velocity from the accelerating potentials. This will not be the case in the rocket since all the ions will enter the spectrometer with the same velocity.

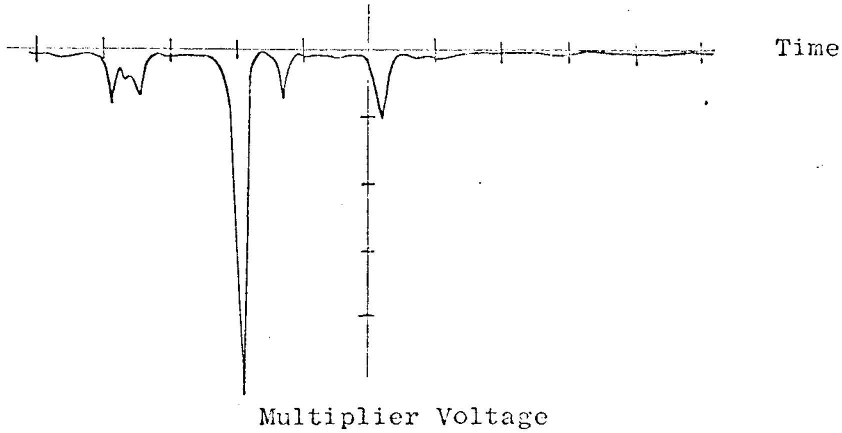

Figure 24
Peaks of (from left to right):
Nitrogen N_1^+ , Water H_2O^+ ,
Nitrogen N_2^+ , Oxygen O_2^+ ,
and argon Ar^+
Obtained with a presure of 2.4 10^{-4} torr
Vertical 50 mV/cm   Horizontal 50 ms/cm

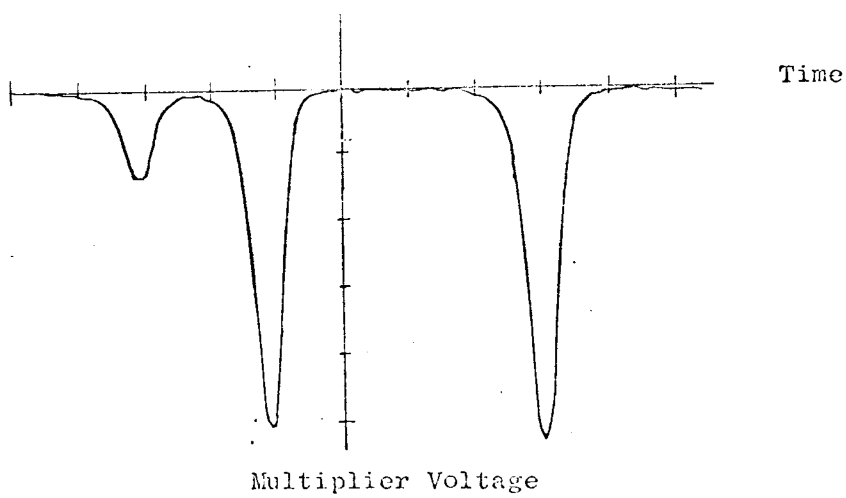

Figure 25
Peaks of Nitrogen, Oxygen and Argon (2.4 10^{-4} torr)
Vertical 50 V/cm   Horizontal 2.5 ms/cm

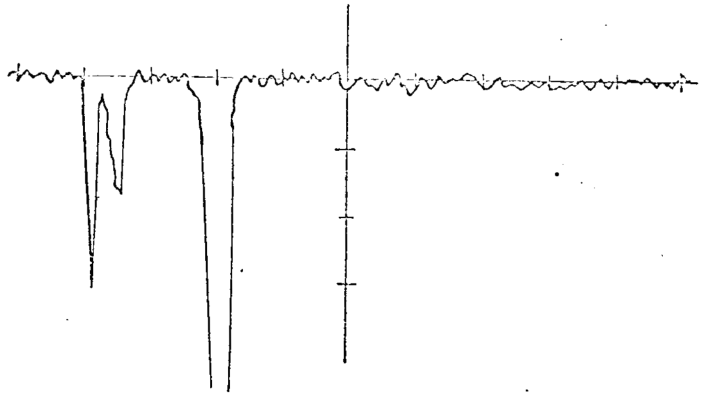

Figure 26
Resolution of N_1^+ and H_2O^+ (2.4 10^{-4} torr)
Vertical 5 mV/cm Horizontal 50 ms/cm

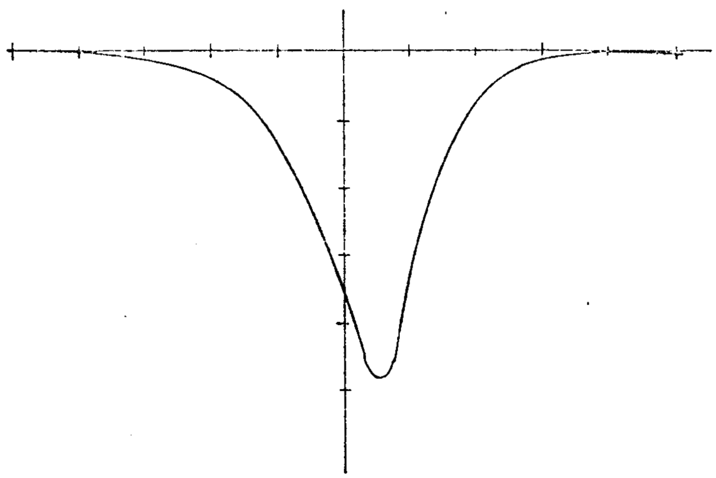

Figure 27
Argon Peak
(2.4 10^{-4} torr Vertical 50 mV/cm Horizontal 5 ms/cm)

The peaks are nearer to each other for lower number because the slope of the sweep is larger at the beginning of the sweep where lower mass numbers are transmitted. On Fig. 26 is a magnified detail from Fig. 24 representing mass numbers 14 and 18.

The resolution was measured from Fig. 25 where the time scale is magnified. The resolution at the 32 peak is 16.7, at 28 peak is 13 and at 40 peak is 21. It can be measured from the figure that the two adjacent peaks will be resolved if the smaller of the two is greater than 10% of the height of the larger. The argon peak with magnified time scale is shown on Fig. 27.

The resolution together with the peak height is a radical function of the D.C. to A.C. ratio which is to be expected and agrees with theory. The D.C. balance to ground does not make noticeable changes due to the fact that the balance potentiometer is small compared to resistors in series with it.

The system is very sensitive to changes in power supply voltage. That is primarily so because that voltage directly drives the oscillator. Therefore, batteries or regulated power supplies have to be used to avoid additional modulation of the high frequency voltage which can bring uncertainty in the results. Considering that the objective of the measurements will be primarily the mass range from 20 to 50, it seems that the instrumentation will be adequate for this purpose.

In further development, the emphasis should be made on miniaturization of components. The number of components in the oscillator can be reduced nearly by a factor of 2 if a monopole mass spectrometer is used. Improvements in resolution can be made by using higher frequencies which will also reduce the size of the coil. However, with a higher frequency the voltage must also be higher in order to cover the needed mass range and this represents a limit when solid state devices are used.

If more accurate results are needed, a frequency modulated oscillator can be used but this inevitably makes the system more complicated.

REFERENCES

1. Brubaker, Wilson, M., and Johannes Tuul, April 1964: "Performance of a Quadrupole Mass Filter," Bell and Howell Research Center, Pasadena, California.

2. Lins, S. J., and M. C. Paul, May 1964: "Solid-State Electric Field Generator for the Monopole Gas Analyzer," Research Division, Univac.

3. Narcisi, R. S., and A. D. Bailey, 1965: "Mass Spectrometric Measurements of Positive Ions at Altitudes from: 64-112 Kilometers," J. Geophys. Res., Volume 70, pg. 3687.

4. Paul, W., and M. Raether, 1955: "The Electric Mass Filter," Zeits fur Physik, Volume 140.

5. Paul, W., H. P. Reinhard, and U. von Zahn, 1958: "The Electric Mass Filter as a Mass Spectrometer and Isotope Separator," Research Report, Zeits fur Phys. Bd 152, pg. 143.

6. Wedemeyer, Rudolf, July 1961: "A Molecular Beam Detector with Electron Impact Ionization and with Four-Pole Mass Filter," Ph. D. Thesis, Rheinishe Friedrich Wilhelm--Universitat--Bonn.

7. General Electric Transistor Manual, 1964.